Spatial Vision, Vol. 22, No. 1, pp. 91–103 (2009)

Also available online - www.brill.nl/sv

Configuration stereopsis: a new look at the depth–disparity relation

WHITMAN RICHARDS *

Massachusetts Institute of Technology, Building 32-364, Cambridge, MA 02139, USA

Received 18 April 2007; accepted 4 October 2007

Abstract—Recovering shape in three dimensions has obvious importance for visual perception. Hence one principal goal for stereopsis should be to recover good estimates of 3D shape. But this is impossible if disparity processing is hardwired, because at different fixation distances a fixed angular disparity will correspond to quite different distance increments. An experiment confirms previous evidence that the disparity computation is not hardwired. Specifically, as fixation distance changes, the perceived relation between depth and disparity changes. The changes are consistent with a remapping that partially preserves the constancy of 3D shape over a wide range of fixation distances.

Keywords: Stereopsis; shape perception; binocular vision; size constancy; surface relief; neural plasticity.

INTRODUCTION

The stereoscopic depth perception of the distance between the point of fixation and any other point in space depends in part on the (angular) disparity between the two retinal images of those points. This relation between depth and disparity has been extensively studied by many (Howard and Rogers, 1995). Most of the early psychophysical work focused on how angular disparity was computed, namely whether zero disparity mapped to positions on a circle through both eyes and the fixation point (i.e. Vieth-Muller circle), or whether zero disparity corresponded to equal apparent directions in the two eyes, or the same frontal-parallel distance as the fixation point (Helmholtz, 1910/1962; Ogle, 1950). Later psychophysical studies, however, recognized that in order to understand better the relation between stereopsis and depth, one might wish to determine the loci of points that lie 10% closer (or farther) than the fixation point (Blakemore, 1970a; Jones, 1974; Lazarus, 1970), or perhaps the locus of depths slanted with respect to the sagittal plane

*E-mail: wrichards@mit.edu

(Blakemore, 1970c; Wilson, 1976), or the curvature of a surface (Bradshaw *et al.*, 1996; Rogers and Bradshaw, 1993; Wildes, 1991). Yet another set of studies have focused on the relation between perceived distance (depth) and the actual viewing distance (Foley, 1967, 1980, 1985, 1991; Ono and Comerford, 1977; Ritter, 1977; Wallach and Zuckerman, 1963). Many experiments, then, have addressed how disparity increments are related to perceived distances or depth. Here, we describe some results that relate to these studies. Specifically our concern is the disparity required to maintain the same 3D configuration (differing only in scale) as fixation distance is changed. Rather than trying to construct a contour-like map of depth *versus* disparity (such as a horopter or its variants), we examine the perceived relation between an object's width (or height) in the frontal plane and its depth along the line of sight. If a principal goal of stereopsis is to assess 3D shape, then binocular vision should provide a consistent measure of the width to depth ratio of an object, regardless of its distance from the observer.

Unfortunately, constant angular disparity referenced to the fixation point will lead to different distance increments as the fixation distance is changed. Because disparities change inversely with the square of fixation distance, but angular size varies only with the inverse of fixation distance, the scaling of a 3D configuration needs to be compensated by a fixation distance factor. Let δ, I, d, W, F and ϕ respectively indicate disparity, the interpupil separation, the extent of the configuration in the sagittal plane (i.e. its 'depth'), the width in the frontal plane, the fixation distance, and the angular width of the display. Then for small angles, simple geometry yields

$$\rho = \frac{d}{W} = \frac{\delta F^2}{IW} = \frac{\delta F}{I\phi}, \tag{1}$$

where ρ is the aspect ratio or surface relief of the object for the particular viewpoint.

If this ratio is to remain constant as fixation distance is changed, then an F/I compensation is needed. Hence an observer judging aspect ratio or surface relief using angular disparities and angular size would require a scaling of I/F with fixation distance. Without such a scaling, as a circle (or triangle) is moved toward the horizon, it will flatten to an ellipse elongated in the frontal plane, and conversely as the circle is moved nearer, it will be elongated in the sagittal plane along the line of sight. Figure 1 illustrates for a triangle. Such changes in configuration would clearly be troublesome, for it means that the shape of objects as measured by stereopsis should undergo drastic distortions as their distance from the observer varies. However, this is not our experience. For example, if we take a cylindrical or spherical object, and move it from 30 to 300 cm, we expect the depth to width ratio to vary by an order of magnitude. Instead, the perceived configuration changes by less than 3 instead of the expected 10. Wallach and Zuckerman (1963) were among the first to confirm this trend to constancy. One implication is that the stereoscopic process is applying some correction to binocular disparities as fixation distance is altered. The following experiment measures the disparity–depth scaling effect, and reveals a relation to the illusory changes of images with fixed angular size (i.e.

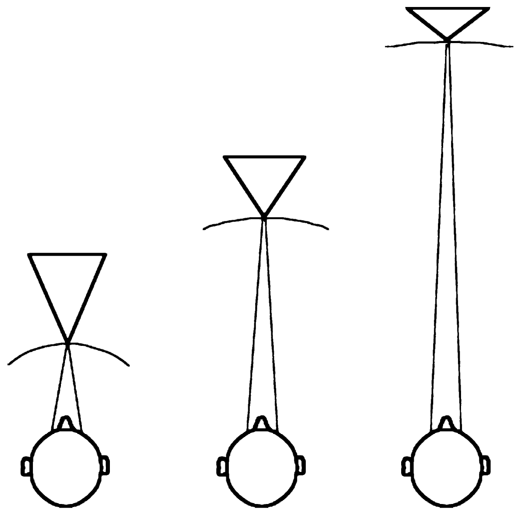

Figure 1. Top view of a plane defined by the two nodal points of the eye and the fixation position. If the center equilateral triangle is moved outwards, then the disparity between its near vertex and its base decreases, leading to the perception of a squashed triangle. Conversely, the triangle should appear elongated if moved inward. The observed shape changes are about half those expected.

a micropsia) that are typically observed during vergence shifts (Duke-Elder, 1939; Helmholtz, 1910/1962; Hollins, 1976).

METHOD

The experimental technique used was a version of the Pulfrich effect, where the frontal positions of points moving to and fro to one eye were delayed with respect to those in the other (Pulfrich, 1922). This creates the illusion of circular or elliptical motion in depth, such as the swinging bob of a pendulum. We used a version of this illusion to assess the perception of 3D shape. In the Pulfrich case, typically only one point (or line) is used. Our modification used three sets of nine points, with each point corresponding to the vertices of a trapezoidal window with four panes. Hence the points were located at the four vertices of, plus the four endpoints of an imaginary vertical and horizontal crossbar, plus the final point of their intersection. Each set of nine points was seen only by one eye, with the outer two sets of three points delayed with respect to the other. The perceptual result was an Ames-like window rotating about a vertical axis defined by the central three points. The use of points only, rather than a line drawing of the window was mandatory in order to reduce monocular cues to depth.

A Macintosh screen was divided in half to create two separate images of the set of nine points forming the rectangular four-pane window rotating symmetrically and at constant angular speed of 1 rps about the vertical axis. Each eye viewed one half of the screen, aided by a septum, with appropriate prisms and lenses used to create optically a virtual fixation distance. (In some cases, we used anaglyphs with accommodative correction — the results are the same.) If one imagines the trajectory of one of the lateral points of a rigid window as viewed from above, this point would normally trace out a circle in the horizontal plane. Thus, the position of the projection of this point in the frontal plane will be a sinusoidal function of the angle of rotation, say α. If the angle α is the same for the displays in both eyes, $\alpha_L = \alpha_R$, and then the phase angle $\Delta\alpha = 0$ and the binocular view will be of a point Q moving laterally to and fro with a sinusoidal motion in the frontal plane (as illustrated by points q'_R and q'_L in Fig. 2). If $\alpha_L \neq \alpha_R$ however, the apparent motion will generally be elliptical (for small disparities). So, for example in Fig. 2, the phase angle $\Delta\alpha$ is about 45 deg for the virtual points p'_R and p'_L, causing the fusion of the corresponding displayed points p_L and p_R to appear at location P. In the special case where the phase angle $\Delta\alpha$ equals the vergence disparity, γ, then the trajectory will be circular (for small γ); otherwise the trajectory will be an ellipse. Specifically, for small γ, the geometry is such that the aspect ratio (or eccentricity) ε of the trajectory will be

$$\varepsilon = \frac{A}{R} = \frac{F\Delta\alpha}{I + R\Delta\alpha}, \tag{2a}$$

$$\gamma \doteq \frac{I}{F}, \tag{2b}$$

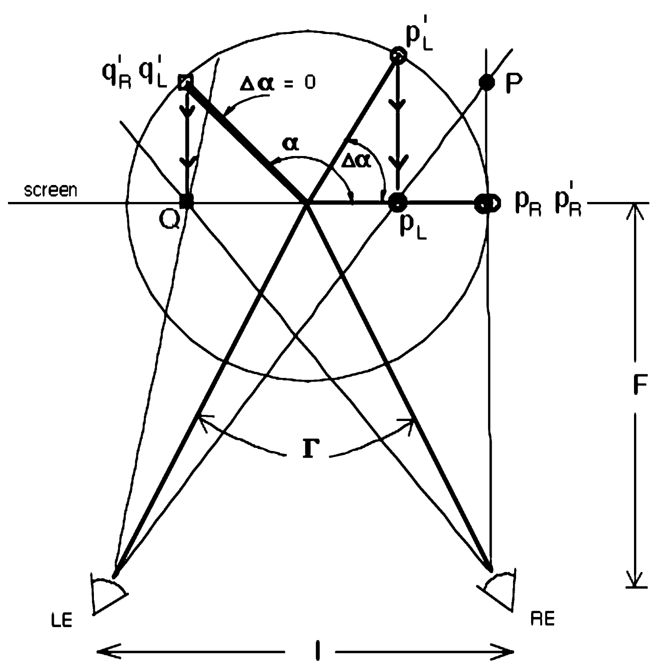

Figure 2. Method of generating elliptical configurations, and notation. P is generated by viewing point p_L in the left eye and p_R in the right. These points oscillate sinusoidally in the frontal plane with the same period, but with a rotational phase angle $\Delta\alpha$ between them. The size of $\Delta\alpha$ determines the aspect ratio of the perceived elliptical motion of a vertical rotating Ames window.

where as before, F is the fixation distance, I the interpupil distance, γ the vergence angle, R is the radius of the reference circle, and A is the distance from the center of the circle to the position of the trajectory along the midline. Note that when $A = R, \varepsilon = 1$, the trajectory is a circle; when $A < R$, the major axis of the elliptical trajectory is R, and when $A > R$, A is the major axis.

The proposed experiment now should be obvious: we simply wish to vary the phase angle $\Delta\alpha$ for a series of fixation distances and determine for each which value generates a circular trajectory of the rotating window. Contrary to the real world situation, in our experimental set-up the frontal extent of the radius R of the circle is held constant, regardless of the fixation distance. Thus, if the angular disparity were hardwired, only one phase angle, say $\Delta\alpha = 0.08$, would be needed to generate the perception of a circular trajectory, and this value would remain the same over all fixation distances. Alternatively, if the phase angle $\Delta\alpha$ for a circle changes, then the relation between depth and disparity must be influenced by vergence. This is the softwired alternative. These two cases lead to easily distinguishable linear relations between $\Delta\alpha$ and fixation distance measured in meter-angles (F^{-1}). The solid curve in Fig. 3 shows the prediction if binocular disparity is hardwired. All measurements of perceived aspect should lie along one curve, varying only with the phase angle $\Delta\alpha$ and not with variations with fixation distance. On the other hand, if the disparity computation completely compensates with fixation distance to preserve 3D shape, then the curves should be displaced with fixation distance, as shown.

Subjects reported perceived aspect ratios of frontal extent to depth (i.e. A/R). Settings for the phase angle $\Delta\alpha$ ranged from 0.01 to 0.40 in at least 1.4× increments for several fixation distances: (∞) (0), 67 (1.5) and 33 (3) cm (meter angles).

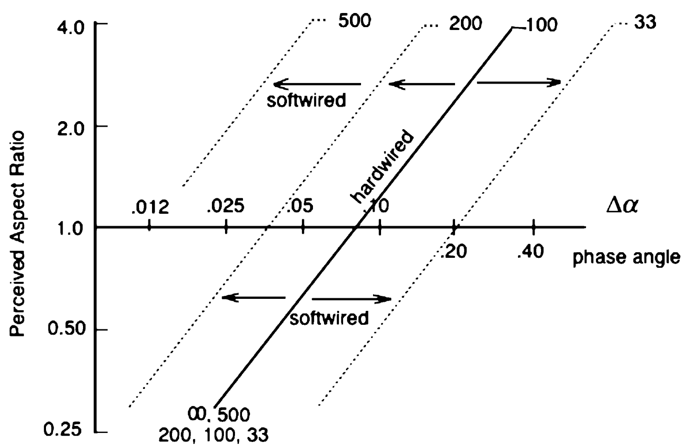

Figure 3. Predicted relations between fixation distance and rotational phase angle for two different models. In the case where disparity is hardwired independent of fixation distance, any given rotational phase angle would elicit the same shape over all fixation distances (heavy solid line). For example if $\Delta\alpha = 0.08$, then regardless of fixation distance, the subject would see a circular trajectory. For a soft-wired system (dotted lines), the angular disparities must be revised as the fixation distance is changed in order that perceptual shape agrees with the true shape.

For WR, additional measurements were also made at $-0.5\ m^{-1}$, which requires divergent eyes and at 133 (0.75) cm. The distance R was typically 2.7 cm, although some measurements that gave similar results were also made with R equal to 0.7 and 5.4 cm. The horizontal width of the trapezoid was 5.4 cm and the height at its midpoint was 4 cm, with the heights of the two vertical sides being 2.6 and 5.4 cm. The pair of stimuli on the Macintosh were separated by 6.4 cm between centers. The standard display was at 67 cm. Because the stimulus separation was equal to the interocular distance, with no prisms the eyes will be parallel and the equivalent fixation distance is infinity $0.0\ m^{-1}$. (Appropriate lenses were added to accommodate this optically.) If the eyes were crossed, then the equivalent fixation distance would be 33 cm ($3\ m^{-1}$). Alternately, this distance could be simulated with the Risley prisms (+lenses) introduced immediately in front of each eye. In this manner, fixation and accommodation were altered without an appreciable change in stimulus angle (the maximum optical magnification is roughly 5%). Some additional measurements were also made with the Macintosh screen placed at either 33 or 133 cm, with the stimulus scaled appropriately. Because there was no significant difference in the measurements for these two other display distances, the data are pooled for each equivalent fixation distance.

RESULTS

For each fixation distance, we obtained the observed aspect-ratio ε for the trajectory of the rotating trapezoid using the equivalent of a range of different angular disparities. The simplest way to present these data is on log–log plots of perceived aspect ratio (ordinate) *versus* the phase angle (abscissa), in other words in the form illustrated in Fig. 3. Thus theoretically we would expect a series of parallel lines each for a different fixation distance, each displaced to intersect the abscissa at a different phase angle. This is illustrated by the set of diagonal dotted lines in Fig. 4 (upper). In contrast, the actual data for 4 observers averaged over individuals and fixation distances appear as open squares through which we have drawn by eye a solid line. The tangent to this solid line for aspect ratios near one has a slope of one-half. Hence perceived aspect is roughly a square root function of phase angle. This result will be used subsequently.

In the lower panel of Fig. 4, we show the slight effect of fixation distance seen in the data of the two subjects on whom extensive measurements were taken. (The author was one of these subjects — the other was naive.) The solid lines through each set of data taken at ∞, 67 and 33 cm are simply a translation of the best-fitting line in the upper panel of Fig. 4. The displacement of these three curves makes clear that some remapping of the relation between phase angle and fixation distance is occurring. However, the displacement in the sets of data is minimal (and also noisy). If we take the intersection of each of these curves with the abscissa where the aspect ratio is 1.0 (circular trajectory), then as shown by the three solid squares in Fig. 5, any putative softwired remapping is roughly halfway to the ideal remapping

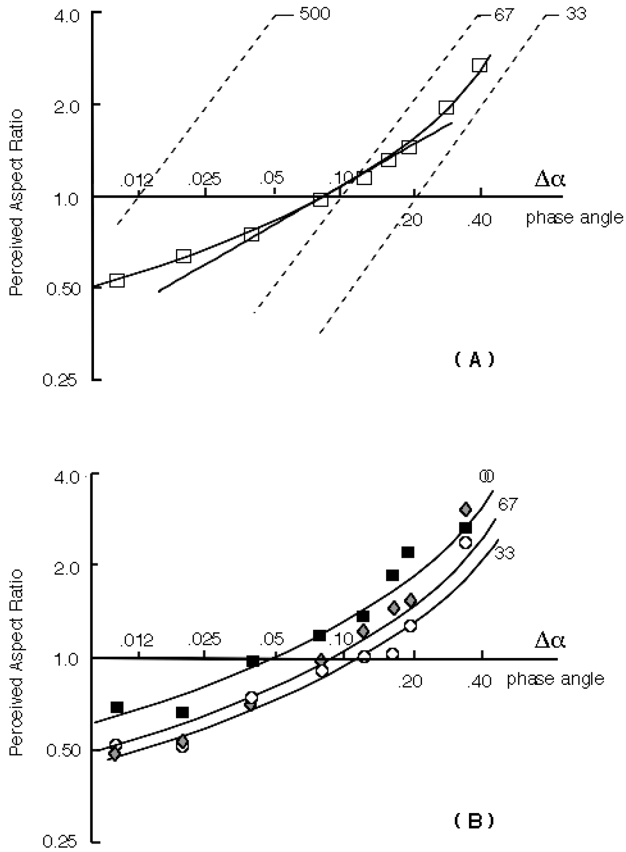

Figure 4. Perceived aspect ratio for a given rotational phase angle $\Delta\alpha$. The dashed lines in the upper panel show the theoretical relation for differing fixation distances based on geometry alone, as if binocular disparity were hardwired, being computed independently of fixation distance. The open squares show the measured aspect averaged over three fixation distances and observers. In the lower panel these 'averaged' data are broken down to show a small effect of changing fixation distance. Note also that the slope of the measured relation between phase angle and aspect is not in agreement with that expected by geometry.

required to preserve shape constancy. This is roughly equivalent to a disparity–depth scaling of $1/F^{1/2}$.

This second result can be plotted in a different way. Again consider only the aspect ratio of 1 corresponding to a circle, and plot $\Delta\alpha$ *versus* fixation distance in meter^{-1} as shown in Fig. 6. (Note inverted ordinate for $\Delta\alpha$.) When fixation is at the horizon, the phase angle $\Delta\alpha$ is about 0.05 and increases to about 0.12 for the nearest fixation distance of 33 cm. First we need to normalize these values to correct for the offset of $\Delta\alpha = 0.05$, which corresponds to the normal vergence resting position (Owens, 1984). Hence $\Delta\alpha = 0.05$ corresponds to 1.0 on the size ordinate (left). For an ideal softwired system, when the rotating configuration is a circle, $\Delta\alpha$ should equal the vergence angle, or equivalently be inversely proportional to meter^{-1}, generating

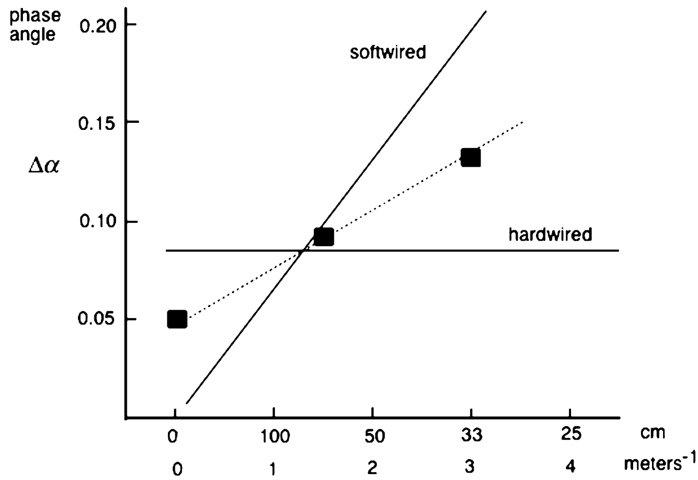

Figure 5. Summary of the predicted relations between fixation distance and the rotational phase angle for a fixed aspect ration for a hardwired and ideally soft-wired model. The solid squares show the measured findings, which lie roughly intermediate between the two extremes.

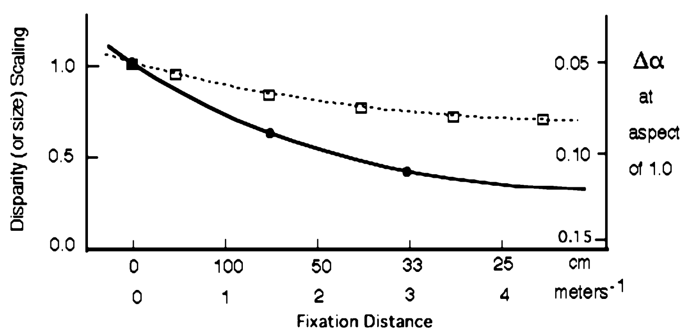

Figure 6. The solid curve shows the required shift in phase angle over fixation distance needed to preserve 3D shape, as measured in this study at three fixation distance. The dotted curve is the classical 'micropsia' size scaling, taken from measurements by Richards (1971b). The proposed model suggests this dotted curve should be the square root of the disparity scaled curve.

a linear relation in Fig. 6. Instead, as we know already from Fig. 5, this is not the case: there is (roughly) a square-root compression. This disparity scaling curve can then be modeled in two ways, with the functions being within 5% of each other over the range studied:

$$\text{scaling} \simeq 1 - \mu(1/F)^{1/2} \tag{3a}$$

$$\simeq \eta/(\eta + F^{-1}), \tag{3b}$$

where F is in meters (or equivalently, F^{-1} are meter angles) and μ and η are constants with respective values of 0.33 and 2.3. Of special interest is that the form of this scaling is very similar to that found for the micropsia or zoom effect for the change in apparent size with fixation distance (Aubert, 1865; Heineman *et al.*, 1959;

Helmholtz, 1910/1962; McCready, 1965). One set of micropsia data averaged over five subjects are shown by the open squares (Richards, 1971b). Note that the size-scaling locus is roughly the square root of the depth scaling. Although the exact compression for both curves in Fig. 6 varies considerably among individuals, their form is always quite consistent. Depth–disparity scaling with fixation distance can be seen as highly correlated with the size-scaling micropsia effect.

DISCUSSION

Our results impact three areas: (1) 3D shape perception (and its developmental aspects); (2) the metric for visual space and (3) the neural mechanism underlying depth–disparity scaling.

First, binocular disparity obviously plays a key role in establishing 3D shape. An ideal machine system could easily rescale disparity with fixation distance to preserve shape aspects. The human mechanism, however, provides only partial compensation over most of the rage of fixation, as shown by Fig. 5. Perhaps, in the presence of other information sources (shading, texture, kinetic depth...) the rough magnitude of disparity scaling is adequate for most perceptual inferences. However, at distances where objects are grasped and manipulated, a crude estimate of 3D aspect may not be sufficient. Hence it is not surprising to see that the depth–disparity relation is most accurate at about 70 cm, which is the average reaching distance for an adult. This possibility immediately suggests that the reference distance for depth–disparity scaling (and 3D aspect) would change as a child develops into an adult. The onset of stereopsis is about ages 2–4 (Fawcett *et al*., 2005; Held *et al*., 1980). The arm length (reach) of a 3 year old grows by a factor of 1.7 from about 40 to 70 cm at age 20 (Konczak and Dichtgans, 1997). Over the same time interval, the interpupil distance increases from 4.8 to 6.0, which is only a factor of 1.25 (MacLachlan and Howland, 2002). Hence the depth–disparity scaling needed is approximately the square-root of the change in reaching distance — roughly as indicated in Fig. 5. Depth–disparity scaling, therefore, could be part of a developmental process with a dynamic carried over to adulthood. Because of the correlation with adult disparity scaling, studies of the development vergence-micropsia illusion in children might elaborate this hypothesis.

The second impact of our results is related to the metrics of visual space. It has been known since 1970 that the micropsia scaling shown in Fig. 6 can account for Ogle's (1950) non-Euclidean variations of the horopter with fixation distance (Jones, 1974; Lazarus, 1970). Although recent results (Hillis and Banks, 2001) contest the earlier variations of the horopter based on corresponding points having the same visual direction, the horopter of greater relevance to disparity scaling uses the apparent frontal-parallel plane as the judged criterion. This judgment is one of depth referenced to the fixation point, or of constant depth planes in the neighborhood of the plane of fixation (e.g. Blakemore's 1970 studies). These latter criteria for horopter measurements suggests a non-Euclidean metric for the depth dimension. Recent experiments by Koenderink *et al.* (2006, 2007) have led to further specifics based on studies of surface shape and relief. They required observers to indicate surface normals at a large number of positions on 2D views of smooth shapes such statues or faces. Given these surface normals, a contour map can be constructed, showing the inferred 3D shape. Several important findings emerged. First, the depth scale of the relief (or surface) varied depending upon whether the viewing was binocular, monocular, or synoptical, where both eyes had same vantage point. (Note that in all three cases, the 2D images had zero disparity.) Yet the nature of the binocular view affected the depth inference. Furthermore, individuals differed in their estimates of the magnitude of the relief of the surfaces. Differences in assumed vantage points also affected the results. Hence we see at least two types of variables in interpreting surface relief: the depth scaling along the line of sight, and two angular variables that specify the viewpoint, namely a slant and a tilt (Stevens, 1983; see also Blakemore, 1970b and Foley, 1972). Based on our observations and those of Foley (1980, 1991) as well as recent results of Koenderink *et al.* (2002, 2007), the inferred metric structure of visual space is consistent with our observations that the depth–disparity scaling is a non-linear dimension independent of slant and tilt. Further support comes from our finding that locally, perceived aspect ε^* is roughly proportional to the square root of the disparity relative to angular size (i.e. Fig. 4A). More specifically,

$$\varepsilon^* = \frac{d^*}{W^*} \propto \left(\frac{\delta}{\phi}\right)^{1/2}, \tag{4}$$

where, as before, δ and ϕ respectively are angular disparity and frontal angular size.

The third impact of our experiments concerns the neural mechanisms underlying depth–disparity scaling. First, Fig. 6 strongly suggests that the classical vergence-micropsia effect is intimately related to disparity scaling. Psychophysical studies have shown that this effect, also called zooming, must be either at or precede the site of binocular interaction (Richards, 1970). Just how this scaling is implemented, however, remains quite unclear. Pouget and Sejnowski (1994) have offered a connectionist-type neural network model that can learn the appropriate scaling. A second type of model proposes a mild shift in the geniculo-cortical mapping such as if different pairs of laminae of the LGN were brought into play as fixation distance is altered (Richards, 1971b). Finally, a third model is one analogous to that used to explain color constancy. We know that there are three classes of binocular disparity pools, each tuned to one of three ranges of disparity: one nearer than the fixation plane, one farther, and the third centered about the plane of fixation (Clarke *et al.*, 1976; Ferster, 1981; Poggio, 1995; Poggio and Fischer, 1977; Richards, 1971a; van Ee and Richards, 2002). Each of these disparity pools has rather broad tuning over disparity. If stereoscopic depth perception is based on the relative activities of these three classes, then depth scaling could be implemented by adjusting these ratios, such as by an inhibition (or excitation) of the pool of disparities centered about the fixation point. All of these models have the minimal neurophysiological support required for plausibility: namely that in monkey and human visual cortex, the activity of some cells are influenced by vergence position (Marg and Adams, 1970; Motter and Poggio, 1990). In addition, some disparity-sensitive cells are found to be active only over a limited range of fixation distances (Gonzalez *et al.*, 2003; Trotter *et al.*, 1992, 2004). (But note that Cumming and Parker, 1999, contest some of these findings.) Furthermore, there is neurophysiological evidence that the lateral geniculate nucleus may be involved. First, vergence movements affect the activity of cells in this nucleus (Donaldson and Dixon, 1980; Lal and Friedlander, 1989; Richards, 1968). Second, the laminar arrangement is attractive for setting up comparisons of angular relations between the two eyes, signed to indicate near or far disparities referenced to the fixation point (McIlwain, 1995; Richards, 1971b). Furthermore, the relative gain of these relations could easily be altered, either by the above-mentioned extra-retinal signal, or by cortical feedback. In sum, given what is known about the cortical-geniculate interactions, these structures become prime candidates for setting up a depth–disparity scaling.

Acknowledgements

John Foley, Jack Beusmans and Richard Wildes provided helpful criticism on early versions of this report, which was kindly presented by Richard Wildes in 2003 at a Symposium in honor of D. M. Regan. Jan Koenderink kindly offered pre-publication findings on the metric space. Early versions of this work was supported by AFOSR 89-504.

REFERENCES

Aubert, H. (1865). *Physiologie der Netzhaut, Raum und Ortsinn III*, pp. 235–251. Morganstern, Breslau, Germany.

Blakemore, C. (1970a). The range and scope of binocular depth discrimination in man, *J. Physiol.* **211**, 599–622.

Blakemore, C. (1970b). The representation of three dimensional visual space in the cat's striate cortex, *J. Physiol.* **209**, 155–178.

Blakemore, C. (1970c). A new kind of stereoscopic vision, *Vision Research* **10**, 1181–1199.

Bradshaw, M. F., Glennerster, A. and Rogers, B. J. (1996). The effect of display size on disparity scaling from differential perspective and vergence cues, *Vision Research* **36**, 1255–1264.

Clarke, P. G. H., Donaldson, I. M. L. and Whitteridge, D. (1976). Binocular vision mechanisms in cortical areas I and II of sheep, *J. Physiol.* **256**, 5006–5026.

Cumming, B. G. and Parker, A. J. (1999). Binocular neurons in V1 of awake monkeys are selective for absolute, not relative disparity, *J. Neurosci.* **19**, 5602–5618.

Donaldson, I. M. L. and Dixon, R. A. (1980). Excitation of units in lateral geniculate and contiguous nuclei of the cat by stretch of extrinsic ocular muscles, *Exper. Brain Res.* **44**, 213–228.

Duke-Elder, W. S. (1939). *Textbook of Ophthalmology*, Vol. 1, pp. 1084. Mosby, St. Louis, MO, USA.

Fawcett, S. L., Wang, Y.-Z. and Birch, E. E. (2005). The critical period for susceptibility of human stereopsis, *Invest. Ophthalmol. Vis. Sci.* **46**, 521–525.

Ferster, D. (1981). A comparison of binocular depth mechanisms in areas 17 and 18 of the cat visual cortex, *J. Physiol.* **311**, 623–655.

Foley, J. M. (1967). Disparity increase with convergence for constant perceptual criteria, *Perception and Psychophysics* **2**, 605–608.

Foley, J. M. (1972). The size-distance relation and intrinsic geometry of visual space: implications for processing, *Vision Research* **12**, 323–332.

Foley, J. M. (1977). Effect of distance information and range on two indices of visually perceived distance, *Perception* **6**, 449–460.

Foley, J. M. (1980). Binocular distance perception, *Psychol. Rev.* **87**, 411–434.

Foley, J. M. (1985). Binocular distance perception: egocentric distance tasks, *J. Exper. Psychol.: Human Perception and Performance* **11**, 133–149.

Foley, J. M. (1991). Binocular space perception, in: *Binocular Vision*, Regan, D. (Ed.), pp. 75–92. Macmillan Press, New York, USA.

Foley, J. M. and Richards, W. (1972). *Perception and Psychophysics* **11**, 423–427.

Gonzalez, F., Justo, M. S., Bermudez, M. A. and Perez, R. (2003). *Neuroreport* **14**, 829–832.

Heinemann, E. G., Tulving, E. and Nachmias, J. (1959). The effect of oculomoter adjustments on apparent size, *Amer. J. Psychol.* **72**, 32–45.

Held, R., Birch, E. E. and Gwiazda, J. (1980). Stereoacuity of human infants, *Proc. Nat. Acad. Sci. USA (PNAS)* **77**, 5572–5574.

von Helmholtz, H. (1962). *Treatise on Physiological Optics*, Vol. 3. (J. P. C. Southall, trans. of 1910 edn). Dover, New York, USA.

Hillis, J. M. and Banks, M. S. (2001). *Vision Research* **41**, 2457–2473.

Hollins, M. (1976). Does accommodative-vergence micropsia exist? *Amer. J. Psychol.* **89**, 443–454.

Howard, I. and Rogers, B. (1995). *Binocular Vision and Stereopsis*. Oxford University Press, Oxford, UK.

Jones, R. (1974). On the origin of changes in the horopter deviation, *Vision Research* **14**, 1047–1049.

Koenderink, J. J., van Doorn, A. J. and Kappers, A. M. L. (2002). Pappus in optical space, *Perception and Psychophysics* **64**, 380–391.

Koenderink, J. J. (2007). *Pictorial Space*. Presentation at MIT, March 2007.

Koenderink, J. J., van Doorn, A. and Kappers, A. (2006). Pictorial Relief, in: *Seeing Spatial Form*, Jenkin, M. and Harris, L. (Eds), pp. 11–32. Oxford University Press, New York, USA.

Konczak, J. and Dichtgans, J. (1997). The development toward stereotypic arm kinematics during reaching in the first 3 years of life, *Exper. Brain Res.* **117**, 346–354.

Lal, R. and Friedlander, M. J. (1989). Gating of retinal transmission by afferent eye position and movement signals, *Science* **243**, 93–96.

Lazarus, M. (1970). A quantitative theory of the horopter. PhD thesis, Department of Brain and Cognitive Sciences, Massachusetts Institute of Technology, USA.

MacLachlan, C. and Howland, H. C. (2002). Normal values and standard deviation for pupil diameter and interpupillary distance in subjects aged 1 month to 19 years, *Ophthal. Physiol. Opt.* **22**, 175–182.

McCready, D. (1965). Size distance perception and accomodation-convergence micropsia: a critique, *Vision Research* **5**, 189–206 (For update see McCready: mccreadd@uwwvax.uww.edu).

McIlwain, J. T. (1995). Lateral geniculate laminations and the corticogeniculate projection: a potential role in binocular vision in the quadrants, *J. Theor. Biol.* **172**, 329–333.

Marg, E. and Adams, J. E. (1970). Evidence for a neurological zoom in vision from angular changes in some receptive fields of single neurons with changes in fixation distance in the human visual cortex, *Experientia* **26**, 270–271.

Motter, B. C. and Poggio, G. F. (1990). Dynamic stabilization of receptive fields of cortical neurons (VI) during fixation of gaze in the macaque, *Exper. Brain Res.* **83**, 37–43.

Ogle, K. (1950). *Researches in Binocular Vision*. W. B. Saunders, Philadelphia, PA, USA.

Ono, H. and Comerford, J. (1977). Stereoscopic depth constancy, in: *Stability and Constancy in Visual Perception: Mechanisms and Processes*, Epstein, W. (Ed.), pp. 91–128. Wiley, New York, USA.

Owens, D. A. (1984). The resting state of the eyes, *Amer. Sci.* **72**, 378–387.

Poggio, G. F. (1995). Mechanisms of stereopsis in monkey visual cortex, *Cerebral Cortex* **3**, 193–204.

Poggio, G. F. and Fischer, B. (1977). Binocular interactions and depth sensitivity in striate and peristriate cortex of behaving rhesus monkey, *J. Neurophysiol.* **40**, 1392–1405.

Poggio, G. F., Gonzalez, F. and Krause, K. (1988). Stereoscopic mechanisms in monkey visual cortex: binocular correlation and disparity selectivity, *J. Neurosci.* **8**, 4531–4550.

Pouget, A. and Sejnowski, T. (1994). A neural model of the cortical representation of egocentric distance, *Cerebral Cortex* **4**, 314–329.

Pulfrich, C. (1922). Die Stereoskopie im Diente er isochromen und heterochromen Photometrie, *Die Naturwissenshaften*, pp. 553, 596.

Richards, W. (1968). Spatial remapping in the primate visual system, *Biol. Kybernetic* **4**, 146–156.

Richards, W. (1970). Oculomotor effects on binocular rivalry, *Psychol. Forsch.* **33**, 136–154 (See also Final report AFSOR 69-1934TR, pp. 122).

Richards, W. (1971a). Anomalous stereoscopic perception, *J. Optic. Soc. Amer*. **61**, 410–414.

Richards, W. (1971b). Size-distance transformations, in: *Zeichenerkenning durch biologische und technisches systeme* (*Pattern Recognition in Biological and Technical Systems*), pp. 276–287. Springer Verlag, New York, USA.

Ritter, M. (1977). Effect of disparity and viewing distance on perceived depth, *Percept. Psychophys.* **22**, 400–407.

Rogers, B. J. and Bradshaw, M. F. (1993). Vertical disparities, differential perspective and binocular stereopsis, *Nature* **361**, 253–255.

Stevens, K. (1983). Slant-tilt: the visual encoding of surface orientation, *Biol. Kybernetic* **46**, 183–195.

Trotter, Y., Celebrini, S., Stricanne, B., Thorpe, S. and Imbert, M. (1992). Modulation of neural stereoscopic processing in primate area V1 by the viewing distance, *Science* **257**, 1279–1281.

Trotter, Y., Celebrini, S. and Durand, J. B. (2004). Evidence for implication of primate area V1 in neural 3-D spatial localization processing, *J. Physiol.* (Paris) **98**, 125–134.

van Ee, R. and Richards, W. (2002). A planar and a volumetric test for stereoanomaly, *Perception* **31**, 51–64.

Wallach, H. and Zuckerman, C. (1963). The constancy of stereoscopic depth, *Amer. J. Psychol.* **76**, 404–412.

Wildes, R. (1991). Direct recovery of three-dimensional scene geometry from binocular stereo disparity, *IEEE Trans. Pattern Anal. Machine Intell.* **13**, 761–774.

Wilson, H. (1976). The significance of frequency gradients in binocular grating perception, *Vision Research* **16**, 983–989.